

Resonance-assisted stabilisation of hydrogen bonds probed by NMR spectroscopy and path integral molecular dynamics

Martin Dračínský,^{a,*} Lucie Čechová,^a Paul Hodgkinson,^b Eliška Procházková,^a Zlatko Janeba^a

^aInstitute of Organic Chemistry and Biochemistry, Flemingovo nám. 2, 16610, Prague, Czech Republic

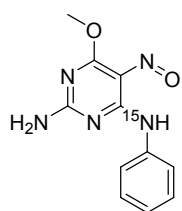
^bDepartment of Chemistry, Durham University, South Road, DH1 3LE, Durham, UK

Supporting Information

Methods

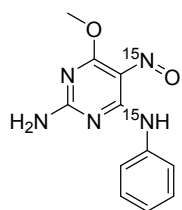
¹⁵N-labelled compounds **1–3** are analogues of previously reported compounds and were prepared by the analogous procedure.¹ Aniline-¹⁵N, ammonia-¹⁵N and sodium nitrite-¹⁵N were used as starting material. 4,6-Dimethoxy-5-(nitroso-¹⁵N)pyrimidin-2-amine for synthesis of compound **3** was prepared by nitrosation using sodium nitrite-¹⁵N.²

6-Methoxy-5-nitroso-*N*⁴-phenylpyrimidin-2,4-diamine-*N*⁴-¹⁵N (**2**)



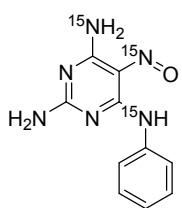
4,6-Dimethoxy-5-nitrosopyrimidin-2-amine (150 mg, 0.8 mmol) was treated with aniline-¹⁵N (83 mg, 0.88 mmol). Compound **2** was obtained as a red solid (151 mg, 77%). ESI MS, *m/z* (%): 247.1 [M + H]⁺; HRMS (ESI) calcd for C₁₁H₁₁N₄¹⁵NO₂ [M + H]⁺ 247.0955, found 247.0954.

6-Methoxy-5-(nitroso-¹⁵N)-*N*⁴-phenylpyrimidin-2,4-diamine-*N*⁴-¹⁵N (**3**)



4,6-Dimethoxy-5-(nitroso-¹⁵N)pyrimidin-2-amine (100 mg, 0.5 mmol) was treated with aniline-¹⁵N (52 mg, 0.55 mmol). Compound **3** was obtained as a red solid (100 mg, 81%). ESI MS, *m/z* (%): 248.2 [M + H]⁺; HRMS (ESI) calcd for C₁₁H₁₂N₃¹⁵N₂O₂ [M + H]⁺ 248.0926, found 248.0927.

5-(Nitroso-¹⁵N)-*N*⁴-phenylpyrimidin-2,4,6-triamine-*N*⁴,*N*⁶-¹⁵N (**1**)



Compound **3** was treated with ammonia-¹⁵N (2M methanolic solution) Compound **1** was obtained as a red solid (40 mg, 44%). ESI MS, *m/z* (%): 234.1 [M + H]⁺; HRMS (ESI) calcd for C₁₀H₁₁N₃¹⁵N₃O [M + H]⁺ 234.0899, found 234.0898.

The NMR spectra were measured at room temperature on a spectrometer operating at 500.0 MHz for ¹H, at 125.7 MHz for ¹³C, and at 50.7 MHz for ¹⁵N in DMSO-*d*₆ (2 mg of the compound

dissolved in 0.6 mL of the solvent) and CDCl_3 solutions were measured on a spectrometer operating at 850.3 MHz for ^1H . The rotamer mixtures of compound **1** were allowed to equilibrate for 24 hours prior to the NMR measurements. The ^{15}N chemical shifts were determined using 1D experiment with direct detection of nitrogens and gated decoupling of hydrogen nuclei. For the assignment of ^{15}N signals based on coupling with directly attached hydrogen atoms, proton coupled nitrogen NMR spectra were also measured. Nitromethane was used as external standard (δ 381.7) for the ^{15}N chemical shifts. Compound **2** and **3** can form one IMHB only, therefore, only one set of signals was found in their NMR spectra.

Born-Oppenheimer and path integral molecular dynamics (PIMD) simulations were run in the CASTEP program,³ which is a DFT-based code, using an *NVT* ensemble maintained at a constant temperature of 300 K using a Langevin thermostat, a 0.5 fs integration time step, ultrasoft pseudopotentials,⁴ a planewave cutoff energy of 300 eV, and with integrals taken over the Brillouin zone using a Monkhorst-Pack⁵ grid of a minimum k-point sampling of 0.1 \AA^{-1} . Electron-correlation effects were modelled using the generalized gradient approximation of Perdew, Burke, and Ernzerhof.⁶ The atomic positions were optimized at the same computational level prior to the MD runs. Both rotamers of compound **1** were modelled as isolated molecules in a cubic periodic box of $20 \times 20 \times 20 \text{ \AA}^3$, and before the production runs of 5 ps were pre-equilibrated by 5 ps (PI)MD simulations to equilibrate the random initial partition of the kinetic energy into rotations, translations and vibrations. The path integral was used on top of the DFT-MD simulations, with a Trotter decomposition of all nuclei into $P = 16$ beads. For the evaluation of deuterium isotope effects, new (PI)MD simulations were performed with the mass of all exchangeable protons (all N–H protons) adjusted to the mass of deuterium. The 10 ps PIMD simulations took ca 10 days on 128 computational cores.

The following procedure was used to calculate the (PI)MD-induced changes of isotropic shielding and deuterium isotope effects. Probability distributions of the N4–H and N6–H bond distances and C4–N4–H and C6–N6–H valence angles were extracted from the (PI)MD simulations. The PIMD distance/angle probabilities were determined independently for all 16 replicas and then averaged. Then a dependence of isotropic shieldings in both forms on the bond distances and the valence angles was calculated by manually adjusting the bond distance in the range $0.8\text{--}1.35 \text{ \AA}$ (with a 0.05 \AA step) and valence angles ranging from 90° to 130° (10° step). These shielding dependencies were calculated using B3LYP functional⁷⁻⁸ and 6-311+g** basis set with the Gaussian09 program⁹ for structures pre-optimised at the same computational level. The calculated dependence of the shielding values on the geometrical parameters was fitted to a quadratic function. The probability distributions and the quadratic functions were then used to calculate weighted averages of shielding values of individual rotamers and for the chemical shift changes induced by the isotope substitution.

The (PI)MD-induced change of isotropic shielding was then calculated as the difference between the averaged NMR parameters and those calculated on a structure with the given distance/angle set to that optimised at the same computational level as used for the (PI)MD simulations.

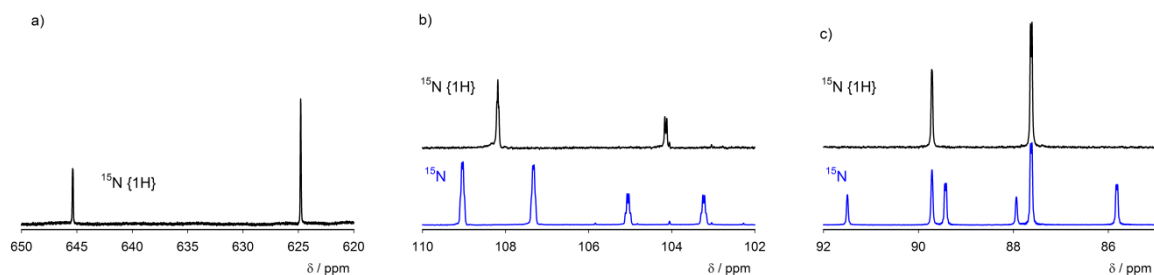


Figure S1. Proton-coupled and proton-decoupled ^{15}N NMR spectra of compound **1**. a) NO region; b) N6 region; c) N4 region.

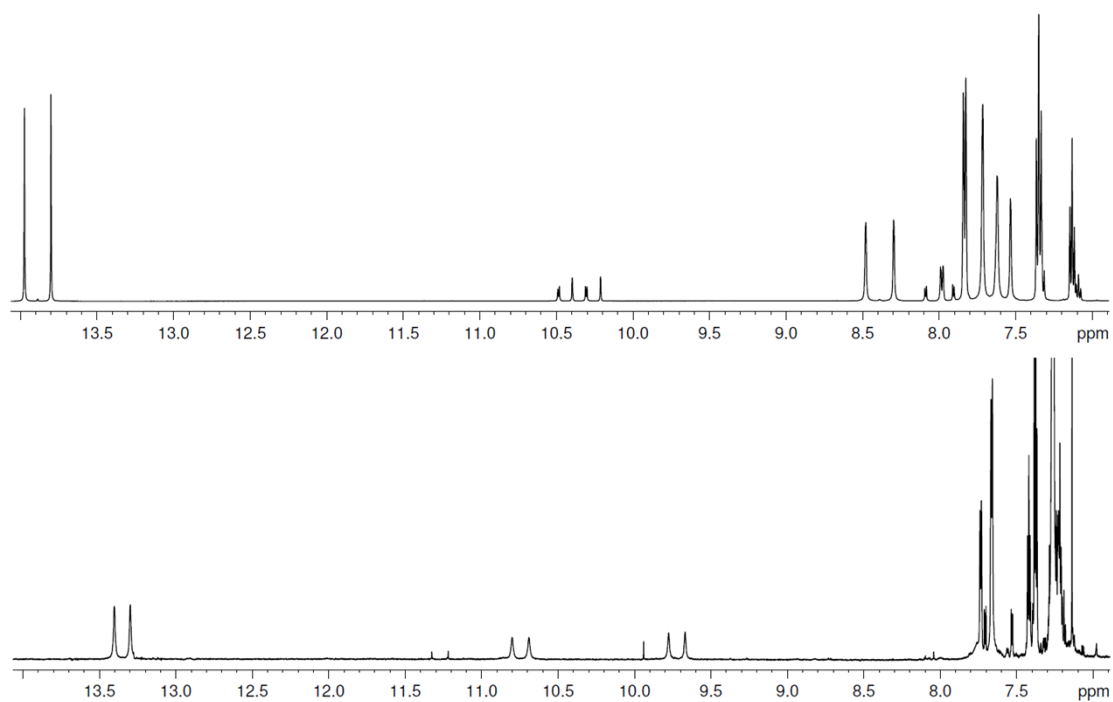


Figure S2. ^1H NMR spectra of compound **1** acquired in DMSO (top, 32 scans, 500 MHz spectrometer) and in CDCl_3 (bottom, 1024 scans, 850 MHz spectrometer).

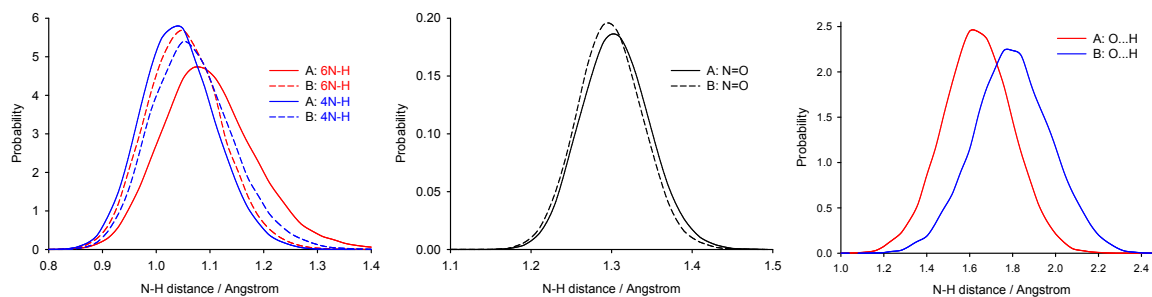


Figure S3. Distributions of probabilities of selected bond distances obtained from PIMD simulations.

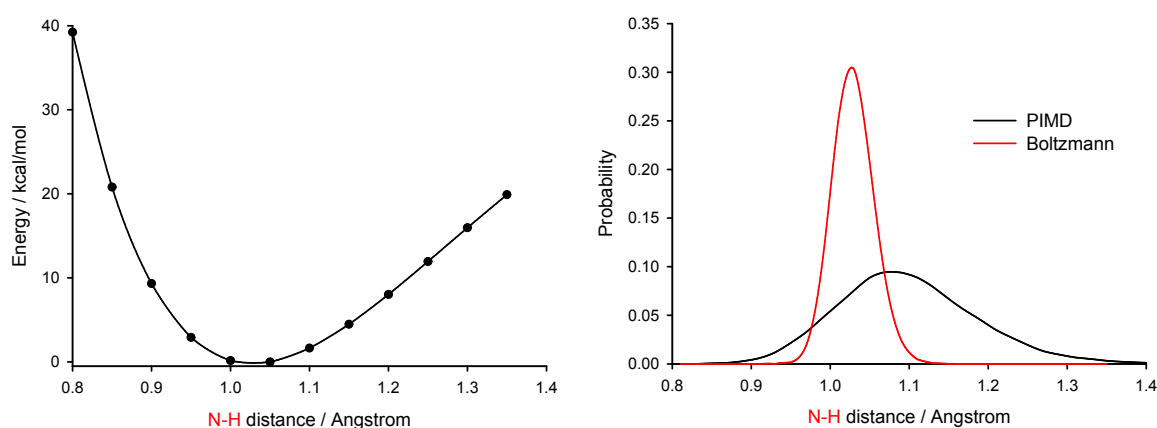


Figure S4. Calculated (B3LYP/6-311+g**) relative energy dependence on 6N-H distance in rotamer **1A** (left) and normalised probability distribution of the N-H distances based on Boltzmann distribution and observed in the PIMD simulation (right).

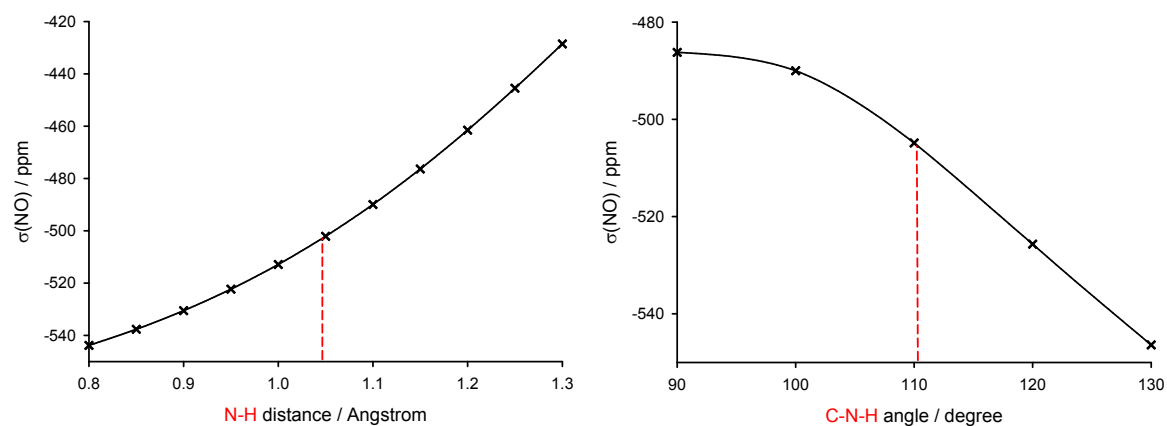


Figure S5. Bond (N6-H) and angle (C6-N6-H) dependence of nitroso nitrogen shielding in rotamer **1A**. The red line indicates the distance/angle in the geometry optimised structure.

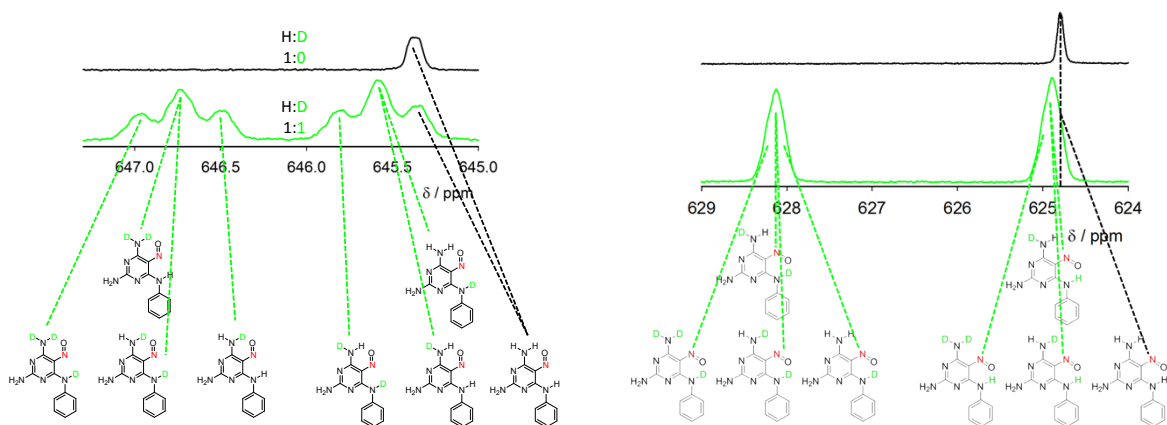


Figure S6. Experimental ^{15}N NMR spectrum (nitroso group region, rotamer **1B** – left, rotamer **1A** – right) of compound **1** in DMSO (black spectrum) and of compound **1** recrystallized from $\text{H}_2\text{O}/\text{D}_2\text{O}$ mixture (1:1) and dissolved in DMSO (green spectrum).

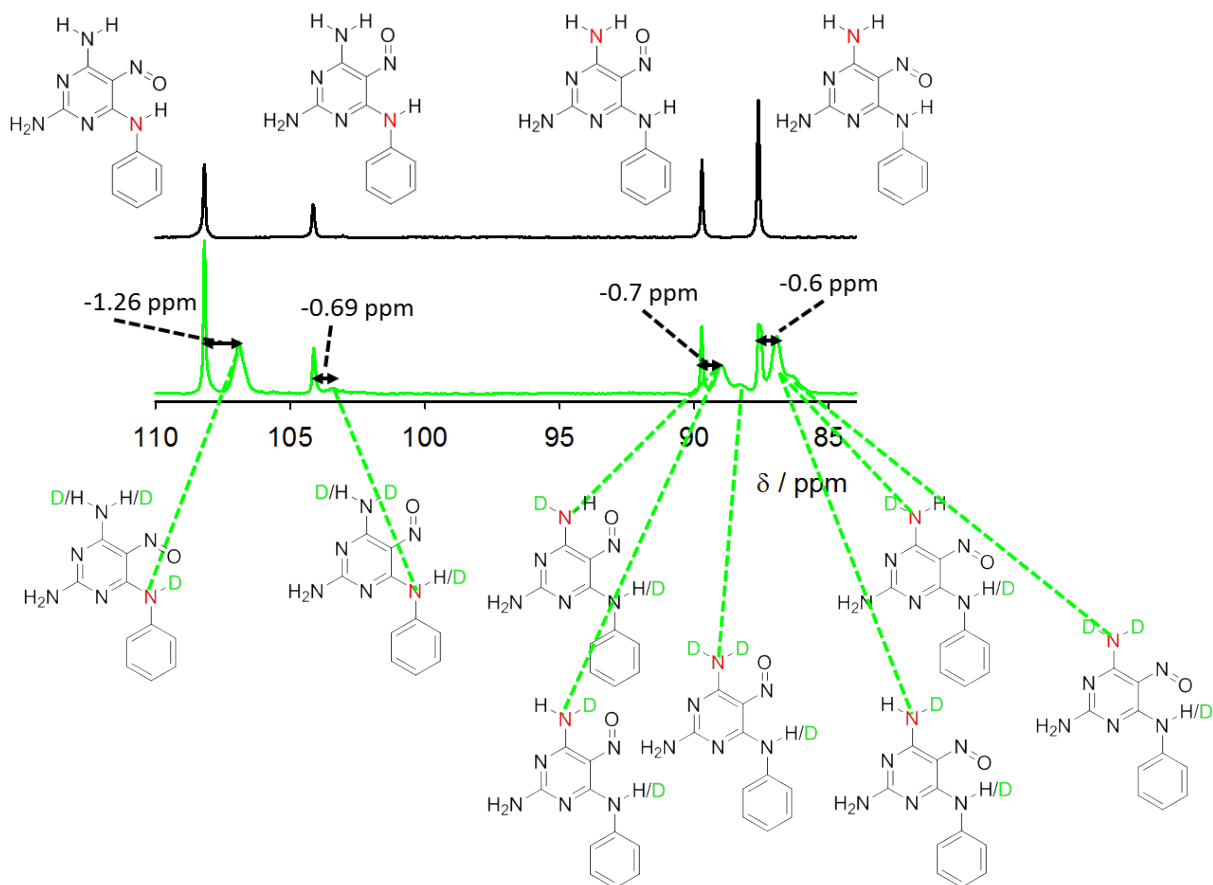


Figure S7. Experimental ^{15}N NMR spectrum (NH group region) of compound **1** in DMSO (black spectrum) and of compound **1** recrystallized from $\text{H}_2\text{O}/\text{D}_2\text{O}$ mixture (1:1) and dissolved in DMSO (green spectrum).

Table S1. Calculated shielding values (ppm) of the nitroso nitrogen in rotamers **1A** and **1B** of compound **1** at different computational levels.

	LDA 6-311+g**	PBE 6-311+g**	B3LYP 6-311+g**	M06 6-311+g**	B3LYP ^a 6-311+g**	B3LYP 6-31g*	Experiment
A	-420.0	-440.2	-507.1	-629.7	-508.2	-441.8	
B	-429.6	-450.7	-517.1	-644.4	-519.7	-447.0	
$\Delta\delta_{(B-A)}$	9.6	10.5	10.0	14.7	11.5	5.2	20.6

^aWith empirical correction for dispersion according to Grimme.¹⁰

Table S2. Calculated shielding values (ppm) of the nitroso nitrogen in rotamers **1A** and **1B** of compound **1**, MD corrections of the nitrogen shieldings calculated by convoluting the bond/angle probability distribution with the shielding surface, and experimental and calculated chemical shift differences between the NO nitrogens in rotamers **1A** and **1B**.

	Static calculation	MD corrections				Total	Experiment
		6N-H	4N-H	C6-N-H	C4-N-H		
A	-507.1	+4.8	+0.2	+1.5	+1.1	-499.6	
B	-517.1	+0.5	+0.7	+0.4	+0.6	-514.9	
$\Delta\delta_{(B-A)}$	10.0					15.3	20.6

Table S3. Average bond distances (angstrom) in pseudorings with RAHB found in (PI)MD trajectories of compound **1** and in geometry optimised structures.

Rotamer	Method	6N-H	4N-H	N-O	C5-N	O...H
1A	PIMD	1.096	1.042	1.305	1.368	1.637
1B	PIMD	1.058	1.066	1.300	1.367	1.789
1A	PIMD-deuterated	1.086	1.039	1.304	1.369	1.651
1B	PIMD- deuterated	1.052	1.059	1.298	1.368	1.800
1A	MD	1.067	1.027	1.298	1.366	1.675
1B	MD	1.040	1.042	1.292	1.365	1.833
1A	MD- deuterated	1.066	1.027	1.298	1.366	1.679
1B	MD- deuterated	1.041	1.045	1.293	1.365	1.803
1A	Optimised	1.046	1.024	1.291	1.364	1.827
1B	Optimised	1.033	1.039	1.290	1.359	1.789

References

1. Procházková, E.; Čechová, L.; Janeba, Z.; Dračínský, M. *J. Org. Chem.* **2013**, *78*, 10121-10133.
2. Jungmann, O.; Pfeleiderer, W. *Nucleosides Nucleotides Nucleic Acids* **2009**, *28*, 550-585.
3. Clark, S. J.; Segall, M. D.; Pickard, C. J.; Hasnip, P. J.; Probert, M. J.; Refson, K.; Payne, M. C. Z. *Kristallogr.* **2005**, *220*, 567-570.
4. Vanderbilt, D. *Phys. Rev. B* **1990**, *41*, 7892-7895.
5. Monkhorst, H. J.; Pack, J. D. *Phys. Rev. B* **1976**, *13*, 5188-5192.

6. Perdew, J. P.; Burke, K.; Ernzerhof, M. *Phys. Rev. Lett.* **1996**, *77*, 3865-3868.
7. Becke, A. D. *J. Chem. Phys.* **1993**, *98*, 5648-5652.
8. Lee, C. T.; Yang, W. T.; Parr, R. G. *Phys. Rev. B* **1988**, *37*, 785-789.
9. Frisch, M. J.; Trucks, G. W.; Schlegel, H. B.; Scuseria, G. E.; Robb, M. A.; Cheeseman, J. R.; Scalmani, G.; Barone, V.; Mennucci, B.; Petersson, G. A.; Nakatsuji, H.; Caricato, X.; Li, X.; Hratchian, H. P.; Izmaylov, A. F.; Bloino, J.; Zheng, G.; Sonnenberg, J. L.; Hada, M.; Ehara, M.; Toyota, K.; Fukuda, R.; Hasegawa, J.; Ishida, M.; Nakajima, T.; Honda, Y.; Kitao, O.; Nakai, H.; Vreven, T.; Montgomery, J., J. A.; Peralta, J. E.; Ogliaro, F.; Bearpark, M.; Heyd, J. J.; Brothers, E.; Kudin, K. N.; Staroverov, V. N.; Kobayashi, R.; Normand, J.; Raghavachari, K.; Rendell, A.; Burant, J. C.; Iyengar, S. S.; Tomasi, J.; Cossi, M.; Rega, N.; Millam, J. M.; Klene, M.; Knox, J. E.; Cross, J. B.; Bakken, V.; Adamo, C.; Jaramillo, J.; Gomperts, R.; Stratmann, R. E.; Yazyev, O.; Austin, A. J.; Cammi, R.; Pomelli, C.; Ochterski, J. W.; Martin, R. L.; Morokuma, K.; Zakrzewski, V. G.; Voth, G. A.; Salvador, P.; Dannenberg, J. J.; Dapprich, S.; Daniels, A. D.; Farkas, O.; Foresman, J. B.; Ortiz, J. V.; Cioslowski, J.; Fox, D. J. *Gaussian 09, Revision A.02*, Gaussian, Inc.: Wallingford CT, 2009.
10. Grimme, S.; Antony, J.; Ehrlich, S.; Krieg, H. *J. Chem. Phys.* **2010**, *132*.